Electronic Supplementary Material (ESI) for Green Chemistry.
This journal is © The Royal Society of Chemistry 2021

Supporting Information

Enzymatic production of β-glucose 1,6-bisphosphate through manipulation of catalytic magnesium coordination

Henry P. Wood,[a] Nicola J. Baxter,[a,b] F. Aaron Cruz-Navarrete,[a] Clare R. Trevitt,[a] Andrea M. Hounslow[a] and Jonathan P. Waltho[a,b,*]

[a]Krebs Institute for Biomolecular Research, Department of Molecular Biology and Biotechnology, The University of Sheffield, Sheffield, S10 2TN, United Kingdom; [b]Manchester Institute of Biotechnology and School of Chemistry, The University of Manchester, Manchester, M1 7DN, United Kingdom

[*]To whom correspondence may be addressed: Prof. Jonathan Waltho, Krebs Institute for Biomolecular Research, Department of Molecular Biology and Biotechnology, The University of Sheffield, Sheffield, S10 2TN, +44 114 22717, j.waltho@sheffield.ac.uk, ORCID 0000-0002-7402-5492

Keywords: glucose bisphosphate | enzymatic production | NMR spectroscopy

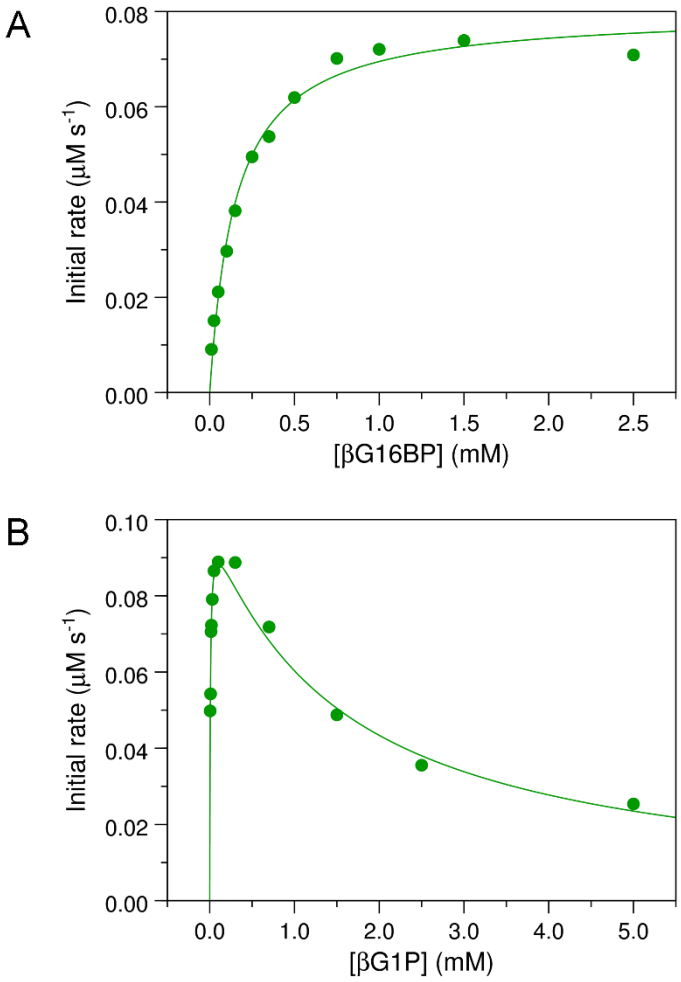

Figure S1. Initial rate measurements for the conversion of βG1P to G6P catalysed by βPGM_{D170N} monitored using a glucose 6-phosphate dehydrogenase (G6PDH) coupled assay. (A) Reactions were conducted in 200 mM K^+ HEPES buffer (pH 7.2), 5 mM $MgCl_2$, 1 mM NAD^+ and 5 U/mL G6PDH containing 10 μM βPGM_{D170N}, 1 mM βG1P and were initiated using increasing concentrations of βG16BP (10, 25, 50, 100, 150, 250, 350, 750, 1000, 1500, 2500 μM). Initial rates of G6P production were obtained using a linear least-squares fitting routine. Subsequent fitting of these rates to Equation 1 using an in-house Python non-linear least squares fitting program yielded an apparent K_m (βG16BP) = 150 ± 13 μM. (B) Reactions were conducted in 200 mM K^+ HEPES buffer (pH 7.2), 5 mM $MgCl_2$, 1 mM NAD^+ and 5 U/mL G6PDH containing 10 μM βPGM_{D170N} and increasing concentrations of βG1P (50, 100, 200, 300, 500, 700, 1000, 1500, 2000, 3000, 5000 μM) and were initiated using 250 μM βG16BP. Initial rates of G6P production were obtained using a linear least-squares fitting routine Subsequent fitting of these rates to Equation 2 using an in-house Python non-linear least squares fitting program yielded an apparent K_m (βG1P) = 6.9 ± 1.0 μM and an apparent K_i (βG1P) = 1536 ± 170 μM.

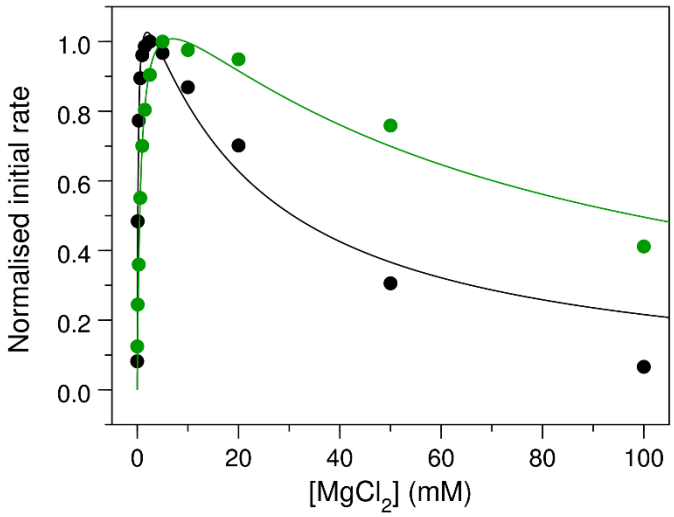

Figure S2. Activity of βPGM_{WT} and βPGM_{D170N} with increasing $MgCl_2$ concentration. Normalised initial rate measurements for the conversion of βG1P to G6P by either βPGM_{WT} (black circles) or βPGM_{D170N} (green circles) at different concentrations of $MgCl_2$ monitored using a G6PDH coupled assay. Reactions were conducted in 200 mM K^+ HEPES buffer (pH 7.2) containing different concentrations of $MgCl_2$ (0, 0.1, 0.3, 0.6, 1.0, 1.5, 2.5, 5, 10, 20, 50 and 100 mM), 1 mM NAD^+, 5 U/mL G6PDH, 1 mM βG1P and either 1 nM βPGM_{WT} with 100 μM βG16BP, or 10 μM βPGM_{D170N} with 1250 μM βG16BP. Initial rates of G6P production were obtained using a linear least-squares fitting routine. Subsequent fitting of these rates to Equation 2 using an in-house Python non-linear least squares fitting program yielded an apparent K_m (Mg^{2+}) = 180 ± 40 μM for βPGM_{WT} and an apparent K_m (Mg^{2+}) = 690 ± 110 μM for βPGM_{D170N}. The standard error of the mean of three technical replicates falls within the radii of the data points. The discrepancy between the K_m (Mg^{2+}) value obtained using the G6PDH coupled assay and ^{31}P NMR time-course experiments (Fig. 3B–C) is likely due to the different conditions employed, although similar maximal initial rates of reaction are observed using each technique (maximal initial rate using G6PDH coupled assay = 0.009 s^{-1}; maximal initial rate using ^{31}P NMR time-course experiments = 0.012 s^{-1}). These observations indicate that a component of the reaction mixture used in the ^{31}P NMR experiments is competing with Mg^{2+} ions to bind to βPGM_{D170N}. One notable difference between the conditions of each technique is the 10-fold higher βG1P concentration used in the ^{31}P NMR experiments. Given that βPGM_{D170N} experiences βG1P inhibition (Fig. S1B) at a comparable level to βPGM_{WT}, this behaviour provides a likely source for the competitive inhibition observed in the ^{31}P NMR experiments. Although the mechanism for βG1P inhibition has not been structurally characterised, it is plausible that βG1P binds to Mg_{cat}-free βPGM_{D170N} to form a closed complex, thus preventing βG16BP production in Step 1 and G6P production in Step 2, until dissociation occurs.

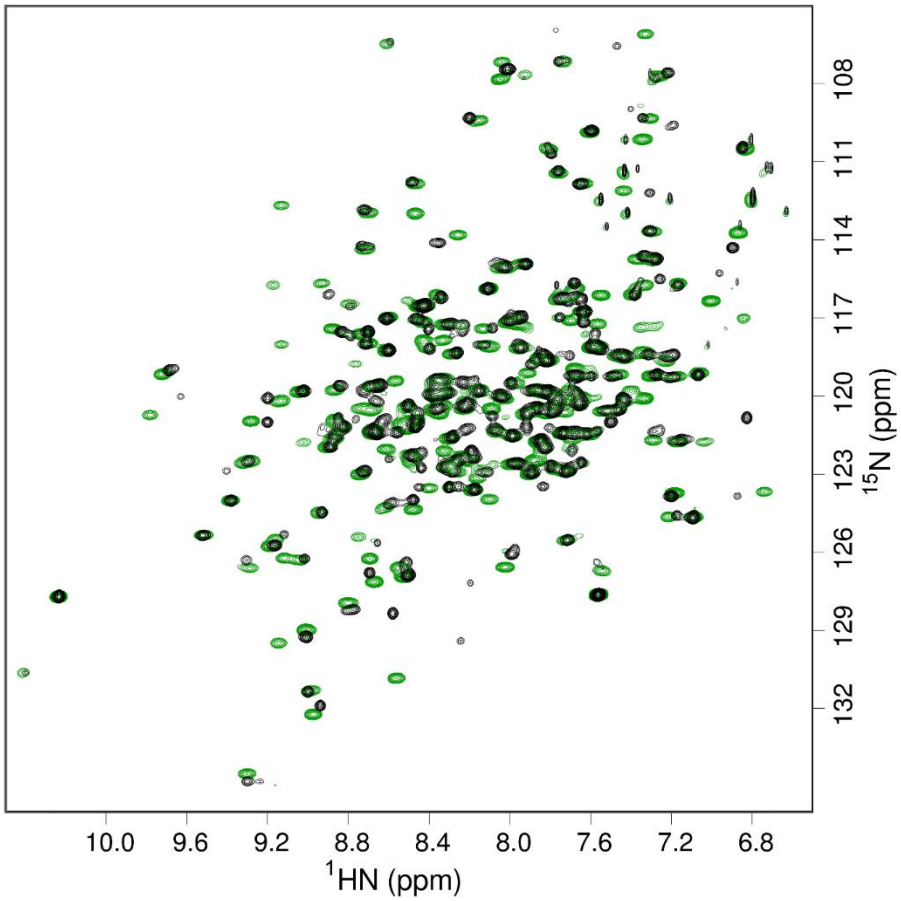

Figure S3. Solution behaviour of substrate-free βPGM. Overlay of $^{1}H^{15}N$-TROSY spectra for substrate-free $βPGM_{WT}$ (black) and substrate-free $βPGM_{D170N}$ (green), recorded in 50 mM K^{+} HEPES buffer (pH 7.2), 5 mM $MgCl_2$, 2 mM NaN_3, 10% $^{2}H_2O$ (v/v) and 1 mM TSP. There is a broad correspondence between peaks of $βPGM_{WT}$ and $βPGM_{D170N}$, indicating a similar solution behaviour and overall protein fold. Two conformers are present in slow exchange (~70% conformer A and ~30% conformer B) for both $βPGM_{WT}$ and $βPGM_{D170N}$, which arise from *cis-trans* isomerisation at the K145-P146 peptide bond.[23] Additionally, ~15 peaks are present for $βPGM_{D170N}$, which are absent in $βPGM_{WT}$ due to backbone conformational exchange on the millisecond timescale.[23] This observation indicates that residue N170 in $βPGM_{D170N}$ abolishes the intermediate exchange dynamic that residue D170 propagates in $βPGM_{WT}$.

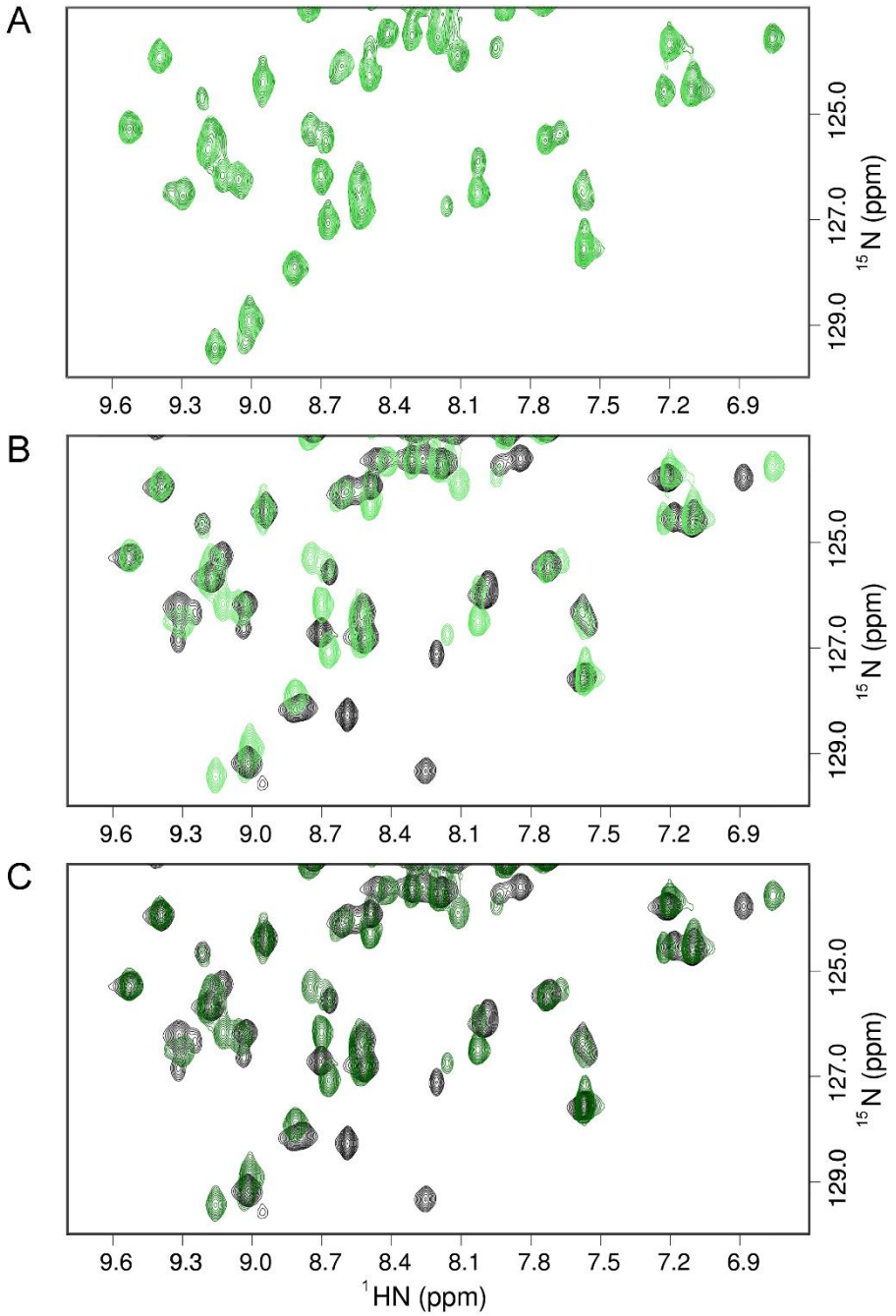

Figure S4. Comparative overlays of a section of $^{1}H^{15}N$-TROSY spectra for substrate-free βPGM recorded in 50 mM K^+ HEPES buffer (pH 7.2), 5 mM $MgCl_2$, 2 mM NaN_3, 10% $^{2}H_2O$ (v/v) and 1 mM TSP. (A) Comparison of substrate-free βPGM_{D170N} that had been preincubated at 25 °C for 0 h (light green) and 48 h (dark green). Near-identical spectra indicate that the incubation process has a negligible effect on the stability of substrate-free βPGM_{D170N}. (B) Comparison of substrate-free βPGM_{D170N} preincubated at 25 °C for 0 h (light green) and substrate-free βPGM_{WT} (black). (C) Comparison of substrate-free βPGM_{D170N} preincubated at 25 °C for 48 h (dark green) and substrate-free βPGM_{WT} (black). The absence of observable βPGM_{WT} peaks in the βPGM_{D170N} spectrum indicates that reversion of βPGM_{D170N} to βPGM_{WT} through deamidation is not a process that occurs readily under these sample conditions.

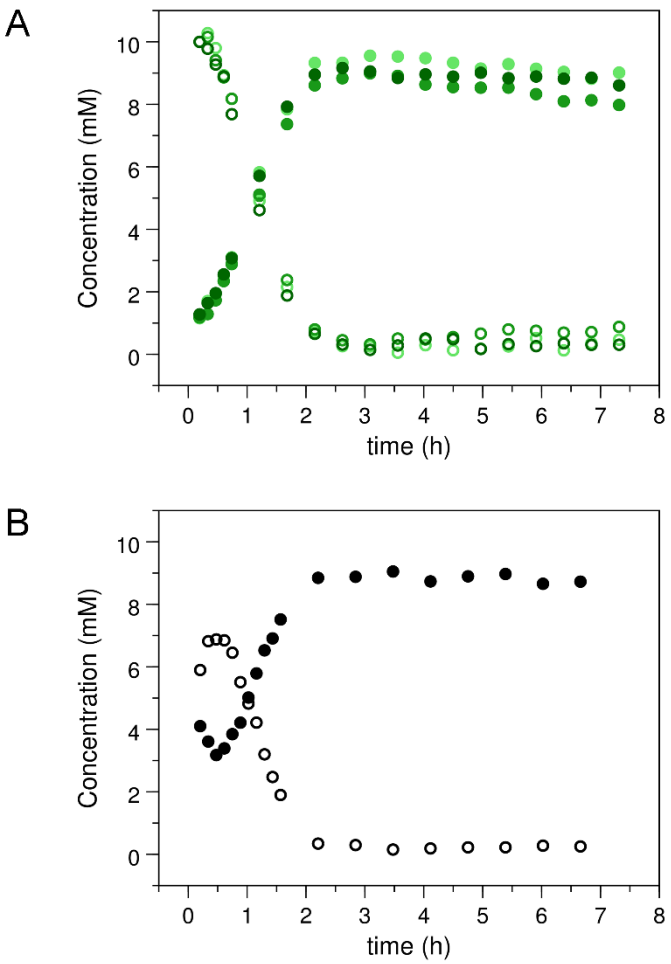

Figure S5. Activity of βPGM_{D170N} in 200 mM K^+ HEPES buffer (pH 7.2) and 100 mM $MgCl_2$ monitored using ^{31}P NMR time-course experiments. (A) Reaction kinetics for the equilibration of 10 mM βG1P with G6P catalysed by 200 μM βPGM_{D170N} that had been preincubated at 25 °C for 0 h (light green symbols), 24 h (medium green symbols) and 48 h (dark green symbols). The reactions were initiated by and timed from the addition of 20 mM AcP. Normalised integral values of the ^{31}P resonances of βG16BP and G6P have been converted to concentrations and are plotted as a function of time for βG16BP (open circles) and G6P (closed circles). (B) Reaction kinetics for the equilibration of 10 mM βG1P with G6P catalysed by 200 μM βPGM_{D170N} containing 200 nM βPGM_{WT} (representative of 0.1% reversion of βPGM_{D170N} to βPGM_{WT} through deamidation). The reaction was initiated by and timed from the addition of 20 mM AcP. Normalised integral values of the ^{31}P resonances of βG16BP and G6P have been converted to concentrations and are plotted as a function of time for βG16BP (open circles) and G6P (closed circles).